

1 **Supplementary Material**

2

3 **A robust initialization method for accurate soil organic carbon
4 simulations**

5

6 Eva Kanari^{1,2}, Lauric Cécillon^{1,3}, François Baudin², Hugues Clivot⁴, Fabien Ferchaud⁵, Sabine Houot⁶,
7 Florent Levavasseur⁶, Bruno Mary⁵, Laure Soucémarianadin⁷, Claire Chenu⁶, Pierre Barré¹

8 ¹Laboratoire de Géologie, École normale supérieure, CNRS, Université PSL, IPSL, Paris, France

9 ²ISTeP, UMR 7193 Sorbonne Université, CNRS, Paris, France

10 ³Normandie Univ, UNIROUEN, INRAE, ECODIV, Rouen, France

11 ⁴Université de Reims Champagne Ardenne, INRAE, FARE, UMR A 614, 51097 Reims, France

12 ⁵BioEcoAgro Joint Research Unit, INRAE, Université de Liège, Université de Lille, Université Picardie Jules Verne, F-02000,
13 Barenton-Bugny, France

14 ⁶UMR ECOSYS, INRAE, AgroParisTech, Université Paris-Saclay, Thiverval-Grignon, France

15 ⁷ACTA - les instituts techniques agricoles, Paris, France

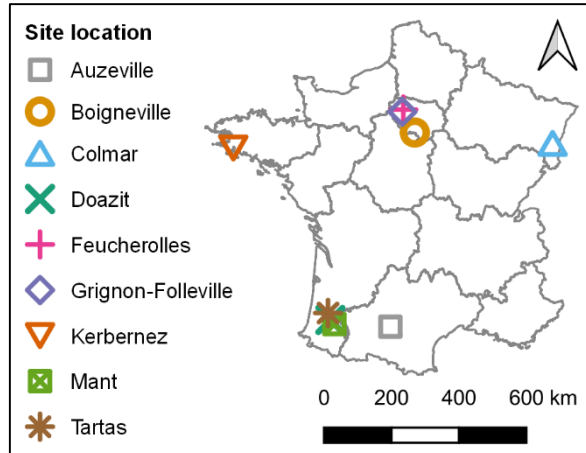
16

17 *Correspondence to:* Eva Kanari (kanari@geologie.ens.fr), Lauric Cécillon (lauric.cecillon@inrae.fr) and Pierre Barré
18 (barre@biotite.ens.fr)

19

20

21



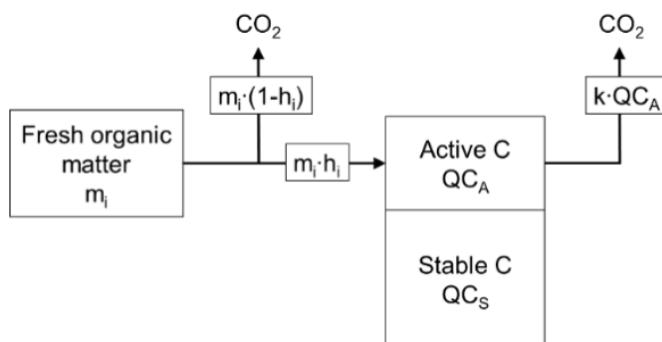
22

23 **Supplementary Material Figure 1: Location of the nine French long-term agricultural experiments used in this study.**

24

25

26



27

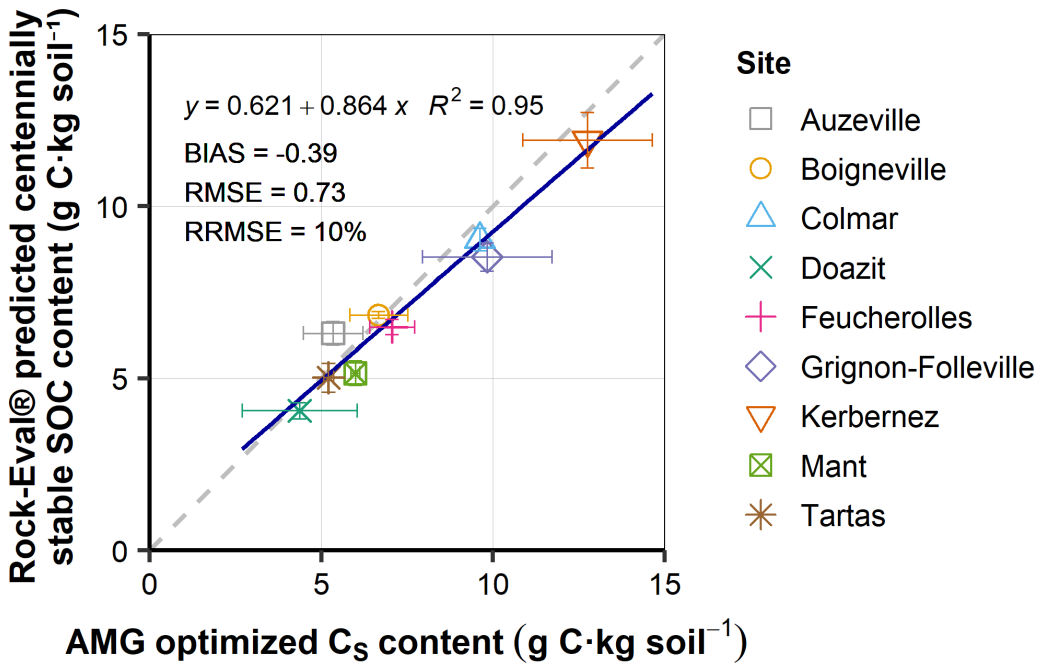
28 **Supplementary Material Figure 2: Conceptual schematic diagram of the AMG model of SOC dynamics (modified from**

29

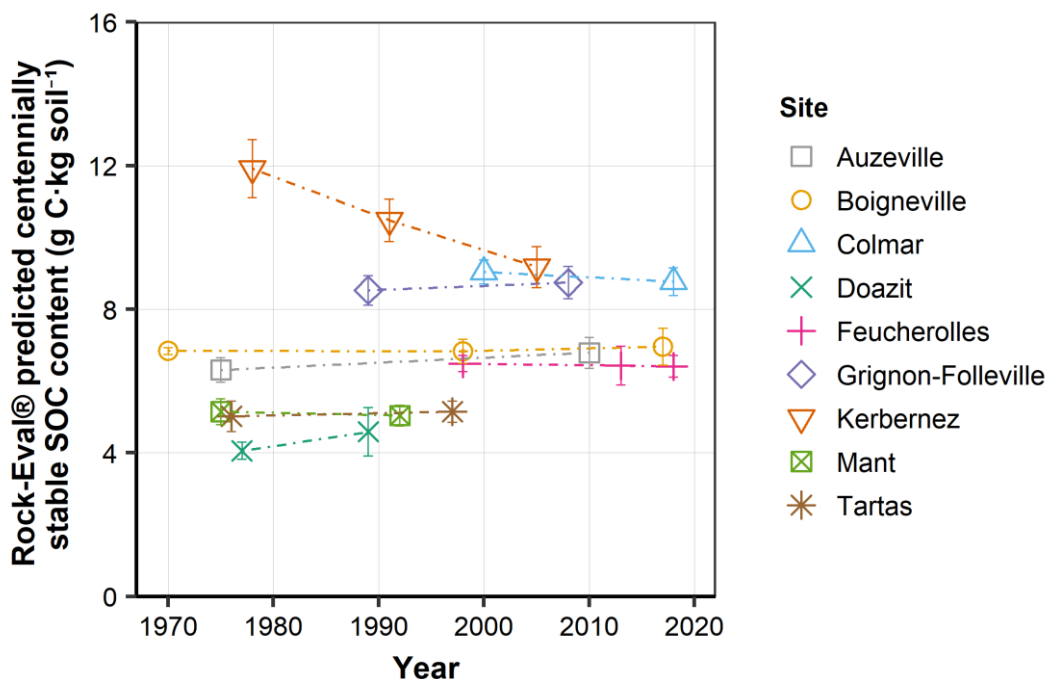
30

31

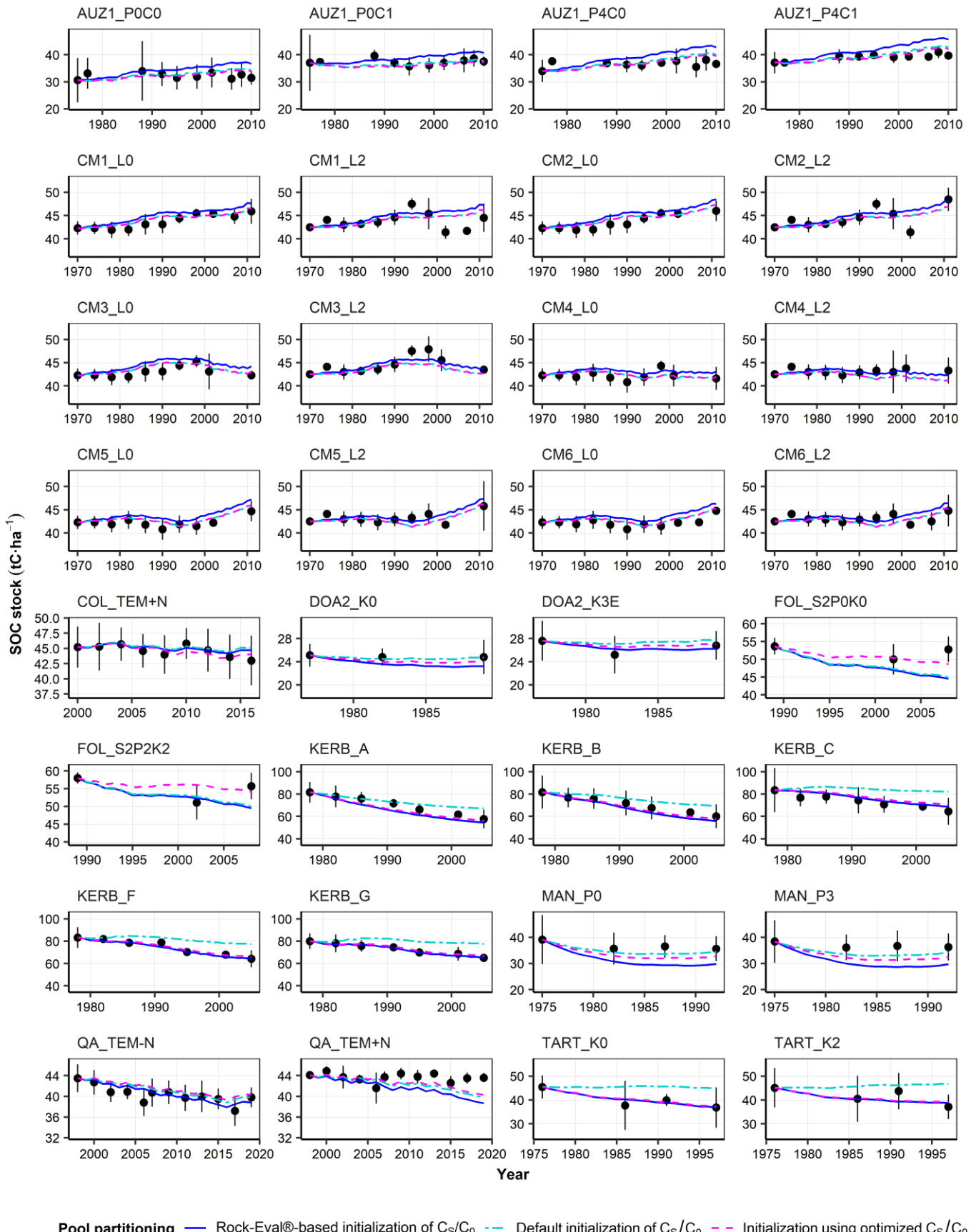
ref^{43,80}), showing SOC pools, fluxes and transport rates. A fraction (1-h) of fresh organic matter (m) is yearly mineralized and released in the atmosphere, whereas a fraction (h) is incorporated into the active SOC pool (C_A). The coefficient of mineralization (k) controls carbon discharge from C_A into the atmosphere. There is no exchange with the stable SOC pool (C_S).



32 Supplementary Material Figure 3: Centennial stable SOC content predicted by the Rock-Eval®-based PARTYsoc
 33 machine-learning model compared to the AMG *ex-post* optimized stable SOC content. Points represent site-mean
 34 values based on initial topsoil samples. Statistics refer to the linear regression between x and y values (blue solid line).
 35 Horizontal error bars show the uncertainty associated with the optimal Cs content, calculated as the standard deviation
 36 of treatment-wise optimized Cs content. Vertical error bars represent the prediction error of the centennial stable
 37 SOC content values, calculated from the standard deviation of the PARTYsoc model predictions on initial topsoil
 38 samples.



40
41 Supplementary Material Figure 4: Centennially stable SOC content predicted by Rock-Eval® as a function of time of
42 the experiment. The points on the plot represent mean values for the shown dates and the vertical error bars represent
43 the standard deviation of the sample set used for averaging. The apparent decrease in centennially stable SOC content
44 for the site of Kerbernez could be explained by changes in soil bulk density, caused by the change in land-use (from
45 grassland to cropland) in 1958. The subsequent soil compaction may have led to inclusion of deeper soil during standard
46 sampling of the 0–25cm layer, causing a false effect of SOC content decrease. Lack of regular soil bulk density
 measurements during the experiment (1978–2005) hinders explicit analysis of this hypothesis.



Pool partitioning — Rock-Eval®-based initialization of C_s/C_0 — Default initialization of C_s/C_0 — Initialization using optimized C_s/C_0

47
48
49
50
51
52

Supplementary Material Figure 5: AMG simulations of observed SOC dynamics for the 32 treatments used in this study. The black points represent observed SOC stocks in topsoils, the vertical error bars indicate the confidence interval of the measurements, and each line corresponds to a simulation resulting from a different initialization method, namely initial pool partitioning according to: Rock-Eval®-based SOC pool partitioning in blue, AMG default C_s/C_0 in cyan, and AMG ex-post optimized C_s/C_0 in magenta. Note the different y-axis range across sites. The treatment IDs and their corresponding sites are presented in Supplementary Material Table 1.

53 **Supplementary Material Table 1: Information on site location, long-term land cover history, climate and soil**
 54 **characteristics. Note that the arable land cover class may include temporary grassland in crop rotations, while the**
 55 **grassland land cover class does not include cultivated crops.**

	Auzeville	Boigneville	Colmar	Doazit	Feucherolles	Grignon-Follevalle	Kerbernez	Mant	Tartas
Latitude ° N	43.527479	48.327843	48.059271	43.700824	48.896501	48.841722	47.946698	43.5917	43.865475
Longitude ° E	1.506059	2.382406	7.328160	-0.629406	1.972125	1.936675	-4.127084	-0.5028	-0.729405
*Historical land cover 1820–1866	arable land	arable land	arable land	grassland					
†Historical land cover 1950–1965	arable land	grassland	arable land	arable land					
‡Treatment									
AUZ1_P0C0	CM1_L0								
AUZ1_P0C1	CM1_L2								
AUZ1_P4C0	CM2_L0								
AUZ1_P4C1	CM2_L2								
	AUZ1_P0C0	CM3_L0							
	AUZ1_P0C1	CM3_L2							
	AUZ1_P4C0	CM4_L0	TEM+N	DOA2_K0	QU_TEM-N	FOL_S2P0K0	KERB_A	MAN_P0	TART_K0
	AUZ1_P4C1	CM4_L2		DOA2_K3E	QU_TEM+N	FOL_S2P2K2	KERB_B	MAN_P3	TART_K2
		CM5_L0					KERB_C		
		CM5_L2					KERB_F		
		CM6_L0					KERB_G		
		CM6_L2							
§MAT (°C)	13.5	10.9	11.2	13.1	10.8	11.0	11.9	13.1	13.4
 MAP-PET (mm)	-290	-87	-222	384	5	-69	489	364	383
Bulk density (g · cm⁻³)	1.40	1.44	1.30	1.40	1.38	1.40	1.30	1.40	1.40
Clay (g · kg soil⁻¹)	275	248	180	72	170	244	163	94	43
Silt (g · kg soil⁻¹)	339	672	628	403	779	601	391	554	166
Sand (g · kg soil⁻¹)	372	80	76	525	51	97	446	349	791
CaCO₃ (g · kg soil⁻¹)	15	0	115	0	0	58	0	3	0
C:N ratio	8.0	9.0	9.2	10.6	9.3	9.8	11.4	9.4	13.0
pH	7.6	6.8	8.3	6.4	6.9	8.1	5.7	7.6	6.0
Reference	ref ⁴⁶	ref ⁴⁷	ref ⁴⁸	ref ⁴⁹	ref ⁵⁰	ref ⁵¹	ref ⁵²	ref ⁵³	ref ⁵⁴

56 * French “Carte de l’Etat Major”, IGN

57 † aerial photography, IGN

58 ‡ Treatments from which samples were available for Rock-Eval® analysis are in bold

59 § Mean annual temperature

60 || Mean annual precipitation-potential evapotranspiration

Supplementary Material Table 2: Measurement error and variation of initial SOC stock values, and variation of initial centennially stable SOC proportion amongst sites. Left part: Comparison of the variation (standard deviation) and uncertainty (confidence interval) associated with initial SOC stock measurements. Right part: variation of initial centennially stable SOC proportions predicted by the PARTYsoc machine-learning model for each site.

Site	Initial SOC stock ($\text{tC}\cdot\text{ha}^{-1}$)			Initial centennially stable SOC proportion predicted using the PARTYsocv2.0EU statistical model	
	Mean	Standard deviation	Confidence interval	Mean	Standard deviation
Auzeville	34.68	2.66	13.30	0.74	0.01
Boigneville	42.40	0.10	2.30	0.68	0.05
Colmar	45.20	-	6.74	0.64	0.02
Doazit	26.35	1.25	5.38	0.57	0.01
Grignon-Folleville	55.85	2.15	3.93	0.64	0.04
Feucherolles	43.80	0.42	3.49	0.62	0.02
Kerbernez	81.98	1.29	24.01	0.44	0.02
Mant	38.75	0.35	17.55	0.52	0.05
Tartas	45.25	0.15	13.14	0.44	0.05